



# Petrological and geochemical characteristics of flood and shield basalts from Kesem-Megezez section, northwestern Ethiopian Plateau: Implication for their mantle source variations

Birhane Girum<sup>a,b,1</sup>, Takele Chekol<sup>a,b,\*</sup>, Daniel Meshesha<sup>a,b</sup>

<sup>a</sup> Department of Geology, College of Applied Sciences, Addis Ababa Science and Technology University, P.O. Box 16417, Addis Ababa, Ethiopia

<sup>b</sup> Mineral Exploration, Extraction and Processing Center of Excellence, Addis Ababa Science and Technology University, P.O. Box 16417, Addis Ababa, Ethiopia

## ARTICLE INFO

### Keywords:

Northwestern Ethiopian Plateau  
Crustal contamination  
Mantle plume  
Alkali basalts  
Transitional basalts  
Kesem Megezez

## ABSTRACT

The Kesem-Megezez Section is located on the western escarpment of the main Ethiopian rift, central Ethiopia, part of the northwestern Ethiopia plateau, and hosts both flood basalts (Kesem Oligocene basalts) and shield volcano basalts (Megezez Miocene basalts) separated by an Oligo-Miocene silicic pyroclastic formation. Petrography, whole-rock trace, and major element data are presented for the Kesem Oligocene and Megezez Miocene basalts to assess their petrogenetic characteristics and the processes involved in their evolution. The Kesem Oligocene basalts are dominated by aphanitic textures, whereas the Megezez Miocene basalts are dominated by porphyritic textures. The Kesem Oligocene basalts are alkaline, whereas the Megezez Miocene basalts have transitional composition. The Kesem Oligocene basalts and Megezez Miocene basalts show distinct compositional differences. MREE/HREE and LREE/HREE show different depths of melt segregation and degrees of partial melting for the Kesem Oligocene basalts and the Megezez Miocene basalts. The geochemical differences (Zr/Nb, Rb/Zr, K/Nb, Ba/Zr and Nb/Zr) between Kesem alkaline basalts and the Megezez transitional basalts reflect the involvement of EMORB-like and OIB-like mantle sources in different proportion in their petrogenesis. Using primitive mantle, garnet- and spinel-bearing lherzolitic sources, a non-modal equilibrium melting model shows that the Kesem alkali basalt can be produced by equilibrium melting of ~3–4% residual garnet and about 3% degree of partial melting. Whereas, the Megezez transitional basalts were formed by melting of ~2–3% residual garnet and >3% degree of partial melting. Geochemical evidences envisioned a scenario in which magmatism started with the arrival of a mantle plume (OIB-like; aka Afar Plume), which comes across a sub-lithospheric geochemically enriched and fertile asthenospheric mantle component (EMORB-like). The upwelling of the hot mantle plume that impinging beneath the lithosphere at ~30 Ma generates OIB-type melts due to decompression. The thermal effect of the hot plume also triggered melting of the fertile E-MORB component in the asthenosphere at the garnet stability depth. Then, the interaction between more melts from the plume (OIB) and lesser melts from the E-MORB created flood basalts (Kesem basalts) in the Oligocene. During the Miocene, the progressive melting of OIB and E-MORB generates the plateau shield basalts (Megezez basalts).

\* Corresponding author. Department of Geology, College of Applied Sciences, Addis Ababa Science and Technology University, P.O. Box 16417, Addis Ababa, Ethiopia.

E-mail address: [takele.chekol@aastu.edu.et](mailto:takele.chekol@aastu.edu.et) (T. Chekol).

<sup>1</sup> Present address: Department of Geology, Collage of Natural and Computational Science, Debre Berhan University, Ethiopia.

<https://doi.org/10.1016/j.heliyon.2023.e17256>

Received 14 December 2022; Received in revised form 10 June 2023; Accepted 12 June 2023

Available online 14 June 2023

2405-8440/© 2023 The Authors. Published by Elsevier Ltd. This is an open access article under the CC BY-NC-ND license (<http://creativecommons.org/licenses/by-nc-nd/4.0/>).

## 1. Introduction

The East African Rift System (EARS) is an active intercontinental rifts extending several kilometers in length with widely distributed bimodal volcanic rocks [e.g., Refs. [1–3]]. The evolution of EARS is attributed to one or two mantle plume(s) [4,5]. The earliest volcanism in the EARS occurred between 40 and 45 million years ago in southwestern Ethiopia and northern Kenya [5–7]. Subsequent volcanism was widespread in Ethiopia and Yemen between 31 and 22 Ma, with continental flood basalts and felsic pyroclastic rocks [1,8–10].

Volcanic rocks of Ethiopia are produced from the upwelling of the mantle plume [11–13]. The Ethiopian volcanic province developed during the Cenozoic, with the eruption of a large volume of continental flood basalt and associated felsic rocks [14]. This volcanic province is one of the largest igneous provinces (LIPs), covering an area exceeding 600,000 km<sup>2</sup> [15]. The volcanic province is classified as Continental Flood Basalt (CFB), shield volcanoes, and rift volcanism [16]. Continental flood basalts erupted during ~30 Ma to form the Ethiopian volcanic plateau [16]. Following the eruption of flood basalts, large shield volcanoes erupted on top of the flood basalts, covering approximately 20% of the plateau [1]. These shield volcanoes (~30–10 Ma) are different from the flood basalts in terms of composition and volume. Shield volcanoes have higher elevations ranging from 1000 to 2000 m above the plateau and are less voluminous [1,15]. Shield volcanoes in the northwestern Ethiopian Plateau include the Simien, Choke, Guguftu, Megezez, and Guna volcanoes [1].

The investigated area, the western escarpment of the MER, is a part of the northwestern plateau of Ethiopia (Fig. 1). The area comprises both flood basalts (Kesem Oligocene basalts; 34 to 30 Ma [17]) and shield volcanoes (Megezez Miocene basalts; 10.5 Ma [2, 18,19]). The study area covers a stratigraphic section (>2000 m) from the Kesem River valley (1267 m) to Mt. Megezez (3509 m), consisting of flood basalts and a shield volcano separated by the Late Oligocene to Early Miocene [17] silicic pyroclastic formation, which is an interesting area to investigate the geochemical nature of both flood basalts and a shield volcano. Therefore, this study focuses on the geochemical compositions and mantle source evolution of the Kesem Oligocene flood basalts and Megezez Miocene shield basalts. This research presents new petrographic and geochemical data and evaluates the role of the asthenosphere, and mantle plume, the contribution of the lithospheric mantle, and crustal materials in the genesis of the flood and shield basalts. Several prior studies have been conducted on the petrology and geochemistry of volcanic rocks in the Ethiopian Plateau, but there are limited geochemical data for the Kesem-Megezez area at the western rift margin of the Main Ethiopian rift, except for studies of volcanic rocks from the Sheno to Megezez [14] and Gina Ager-Megezez volcanic sections [20].

## 2. Geological setting

### 2.1. Ethiopian continental flood basalt (CFB)

The Ethiopian LIP is a recent outpourings of continental flood volcanism related to the EARS crustal extension, including the MER and Afar Rift [1,9,10,14,21,22]. The erupted volcanic display temporal and spatial compositional variations due to different mantle

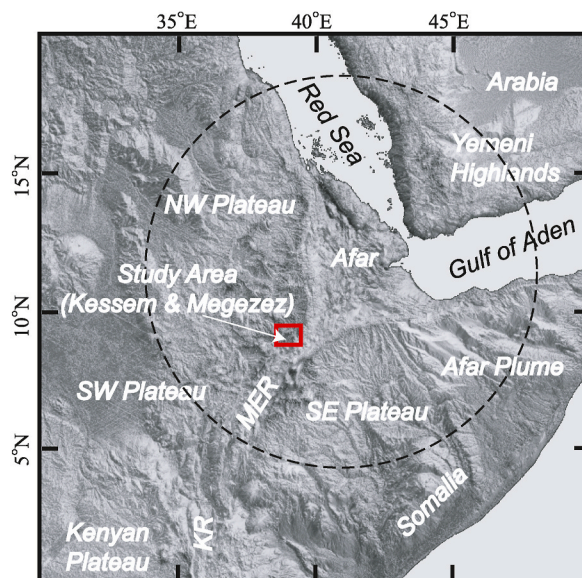


**Fig. 1.** Shaded relief map of East Africa and Arabia (NASA SRTM30) illustrating the position (Main Ethiopian Rift = MER, Kenyan Rift = KR), as well as the Ethiopian and Yemeni plateaus which surround the Afar depression. The circle dash line indicates the extent of Afar plume. The location of study area site is also indicated by red box. (For interpretation of the references to color in this figure legend, the reader is referred to the Web version of this article.)

source contributions [23]. The continental flood basalts of Ethiopia are characterized by tholeiitic and alkaline rocks [1,24]. Zanettin [25] stratigraphically divided Ethiopian plateau volcanism into four secessions, i.e., Ashange basalt (pre-Oligocene), Aiba basalts (34–30 Ma), Alajae basalts and rhyolite (30–26 Ma), and Termaber basalts (Miocene). Later, the northwestern Ethiopian flood basalts were classified into low-Titanium basalts (LT-type) and high-Titanium (HT1- and HT2-type) basalts based on their titanium (Ti) contents [8,9].

## 2.2. The Main Ethiopian Rift

The MER is part of the EARS, connecting the Afar rift in the north with the Turkana depression in the south [2]. It is a volcanic-type rift showing all rift formation stages starting from early continental extension to continental break-up [26]. The MER is mostly subdivided into northern, central, and southern segments with northward rift propagation. The northern MER stretches southward from the Afar Rift to the Koka Lake region and is separated from the central MER by the Boru Toru ridge [27]. The central and southern MER are separated by a Goba-Bonga transverse lineament [27].

The study area (Kesem-Megezez section) is part of the northwestern Ethiopia Plateau and the western escarpment of the MER, covered by volcanics mainly basaltic and pyroclastic rocks (Fig. 2). The lithology of the area consists of basaltic lavas, basaltic scoria, and various welded silicic pyroclastic deposits. The study area comprises 2342 m thick volcanic sequences (from Kesem river valley 1267 m to Mt Megezez 3509 m). The Kesem basalts are exposed near the Kesem River along the main asphaltic road from Arerti to Shola Gebeya. It is intensely fractured, irregularly to columnar-jointed, spheroidally weathered, and forms cliffs (Fig. 3). It is characterized by different phases of basaltic flows separated by randomly exposed paleosols (~20 cm thick). It has a dark fresh color with aphanitic and vesicular textures (Fig. 3a and b). Kesem basalts are commonly aphyric, and rarely porphyritic or glomero-porphyritic. Moreover, pyroclastic deposits, such as ash and tuff, are intercalated towards the top. The general thickness of the Kesem basalts is approximately 690 m, ranging from elevations 1267 m at the Kesem riverbed to 1957 m at the base of the ignimbrite unit. The ignimbrite overlies the Kesem basalts. The fresh color is light grey. The tuff and ash deposits are intercalated with the ignimbrite in different locations (Fig. 3c and d). The silicic pyroclastic formation is, on average, 73 m thick (1957–2030 m elevations) with variable thicknesses at different locations. The Megezez shield basalts overlie the silicic pyroclastic formation. The Megezez shield basalts occupy highly elevated and cliff-forming areas characterized by a slope angle of ~5°. It has sharp contact with the underlying silicic pyroclastic formation. The Megezez shield basalts have an approximate thickness of 1479 m (from 2030 m to 3509 m elevation). At certain locations, the Megezez shield basalts were cut by basaltic dikes (Fig. 3f). It comprises fine, dark grey (fresh color) with an aphanitic, vesicular to porphyritic texture (Fig. 3e and f). The porphyritic basalt is characterized by up to 5 mm large plagioclase phenocrysts and less common aphyric basalts.

## 3. Petrography of basalts from Kesem-Megezez section

### 3.1. Kesem flood basalt (Oligocene)

The Kesem basalts are characterized by their aphyric texture with a minor amount of plagioclase phenocrysts (Fig. 4a–c). The

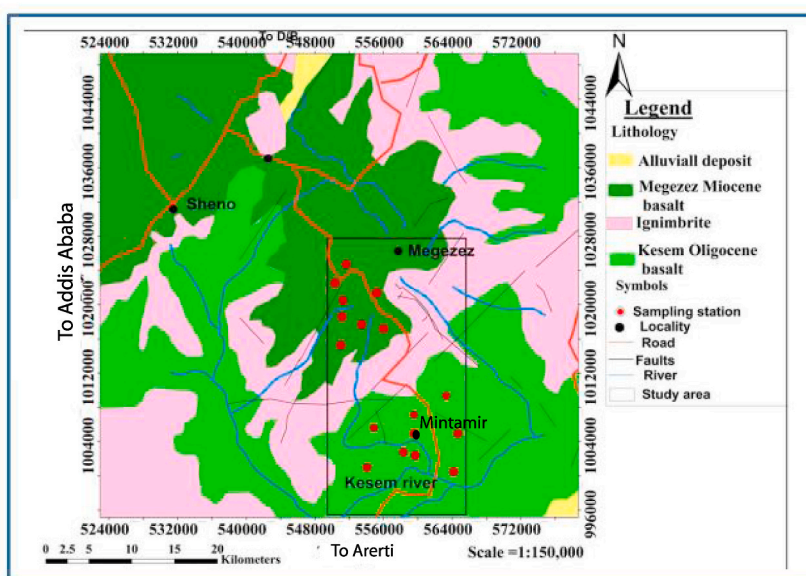
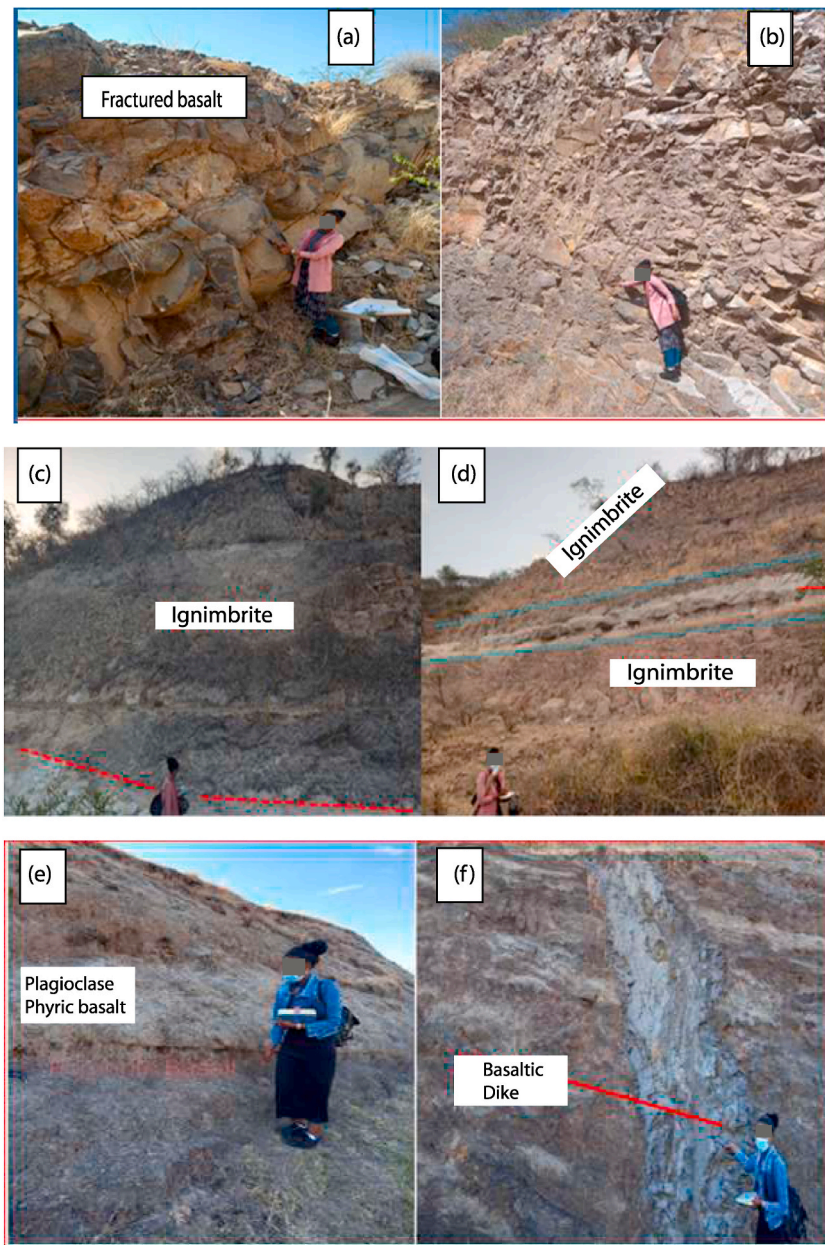


Fig. 2. Geological map of the study area and its surroundings taken from Ref. [48].



**Fig. 3.** A and B) outcrops of Kesem basalt, C and D) ignimbrite, E and F) Megezez basalts.

phenocrysts are  $<1\%$ , and the groundmass is composed of plagioclase, olivine and opaque minerals (KB19). The groundmass consists of equigranular grains with an intergranular texture (KB 8). Most samples of Kesem basalts have a holocrystalline texture. The Kesem basalt KB 16 sample contains plagioclase and opaque minerals as phenocrysts. These basaltic samples contain  $\sim 3\%$  phenocrysts of plagioclase minerals within a groundmass composed of microliters, cryptocrystalline and glassy materials. The plagioclases are euhedral to subhedral with a grain size of up to 2 mm.

### 3.2. Megezez shield basalts (Miocene)

The Megezez basalts are phyric in texture, with phenocrysts of clinopyroxene, olivine, and plagioclase set in intergranular and intersertal textured groundmasses of olivine, plagioclase and opaque minerals. Based on their major phenocryst contents, plagioclase phyric, olivine-pyroxene phyric and pyroxene-phyric basalts are observed in the Megezez basalts (Fig. 5). The plagioclase-phyric basalt consists of up to 4% plagioclase phenocryst (MB3). The size of plagioclase phenocryst ranges from 1 to 4 mm. The groundmass is holocrystalline in texture and contains olivine, plagioclase and opaque minerals. The olivine pyroxene-phyric basalt has olivine and

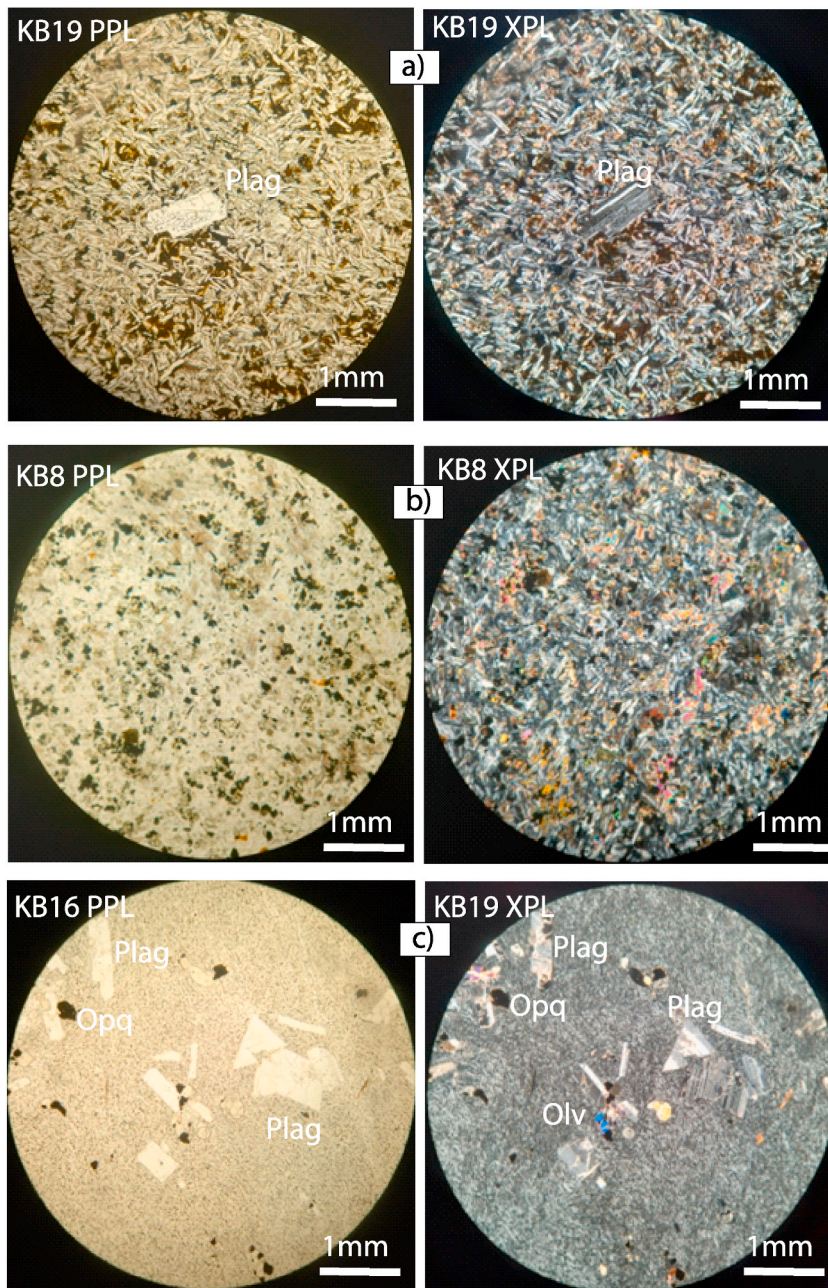


**Fig. 4.** Selected representative photomicrographs of Kesem Basalts. In Plane Polarized Light (PPL) and Cross-polarize (XPL). 4× magnification.

pyroxene as the major phenocrysts, with a holocrystalline texture (MB8). Olivine is altered to iddingsite. It consists of approximately 10% phenocrysts within the groundmass of plagioclase, opaque, pyroxene and olivine minerals. The sizes of olivine and clinopyroxene phenocrysts ranging from 1 to 4 mm. The pyroxene-phyric basalt shows pyroxene as the major phenocryst (~4%). The groundmass contains olivine, pyroxene, and plagioclase with a holocrystalline texture (MB11). The size of the clinopyroxene phenocrysts ranging from 1 to 3 mm.

#### 4. Analytical method

Ten representative samples were sent to the Australian Laboratory Service (ALS) to determine major and trace element contents. Sample preparation was done at ALS Geochemistry, Addis Ababa. 0.20 g of the sample powder was added to 0.90 g of lithium tetraborate flux, and the mixture was homogenized and fused in a furnace at 1000 °C. The resulting melt was cooled and dissolved in 100

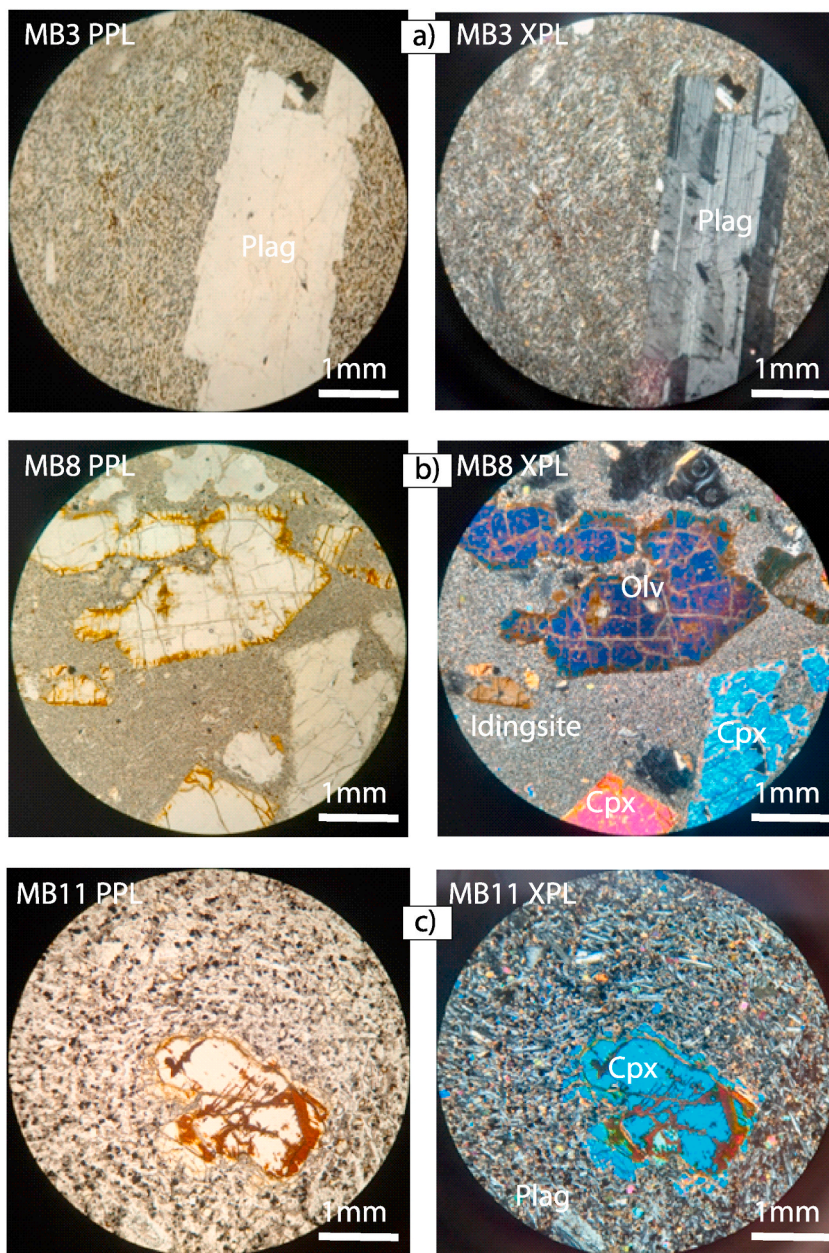


**Fig. 5.** Selected representative photomicrographs of Megezez Basalts: a) plagioclase phyric basalts, b) olivine-cpx phyric basalts and c) cpx phyric basalt. In Plane Polarized Light (PPL) and Cross-polarize (XPL). 4× magnification.

mL of 4% nitric acid/2% hydrochloric acid. The solution was then analyzed using Inductively Coupled Plasma-Atomic Emission Spectroscopy (ICP-AES) and Inductively Coupled Plasma-Mass Spectroscopy (ICP-MS) for major and trace elements, respectively (Tables 1 and 2). A Gravimetric analytical technique was used to determine the loss on ignition (LOI).

Repeatability of the data was checked using duplicate analysis, and accuracy of the data was checked by international rock standard samples (OREAS102a; <https://www.oreas.com/crm/oreas-102> and AMIS0304; <https://amis.co.za/wp-content/uploads/AMIS0304-Certificate.pdf>). The accuracies of major and trace elements are mostly better than 1–2% and 5%, respectively.

## 5. Whole rock geochemistry

### 5.1. Geochemical classification

Based on the Total Alkali versus Silica (TAS) plot, the Kesem Oligocene basalts and Megezez Miocene basalt samples fall in the

**Table 1**  
Major oxide and CIPW normative data for rock samples from Kesem-Megezez Section.

Type	Kesem alkali basalt				Megezez							Standard (this analysis)	
					Transitional basalt				Trachy-andesite				
Sample no	KB9	KB12	KB13	KB14	MB3	MB7	MB10	MB11		MB1	MB4	OREAS 102a	AMIS0304
<b>Easting (m)</b>	564,823	557,343	558,123	564,525	552,925	551,123	553,947	553,590		554,725	553,905		
<b>Northing (m)</b>	1,004,655	1,005,259	1,007,110	1,009,462	1,021,113	1,017,885	1,024,135	1,019,203		1,017,999	1,020,806		
<b>Elev. (m)</b>	1720	2129	2193	2427	3026	3019	3395	3420		3078	3007		
SiO <sub>2</sub> (wt%)	47.1	45.8	46.9	45.7	49.1	45.6	48.8	45.6		57.8	61.7	65.3	12.5
Al <sub>2</sub> O <sub>3</sub>	15.55	16.15	16.35	15.9	15.6	14.95	14.9	14.7		15.9	16.1	12.25	1.52
Fe <sub>2</sub> O <sub>3</sub> *	14	14.65	14.55	14.9	14.8	14.65	14.55	14.75		8.55	6.79	7.99	21.5
CaO	7.29	8.03	8.08	7.98	6.85	11.15	8.58	10.85		4.59	3.33	1.96	28.8
MgO	4.92	5.83	4.98	5.91	2.78	6.96	4.07	7.06		1.7	0.77	2.23	2.87
Na <sub>2</sub> O	3.64	3.32	3.55	3.26	3.86	2.51	3.53	2.6		4.87	5.03	0.14	0.1
K <sub>2</sub> O	1.54	1.46	1.28	1.18	1.52	0.76	1.24	0.76		2.53	3.11	4.34	0.26
TiO <sub>2</sub>	3.37	3.6	3.4	3.42	3.45	2.84	3.49	2.76		1.76	1.52	0.28	1.78
MnO	0.18	0.18	0.18	0.18	0.18	0.19	0.19	0.18		0.17	0.17	0.06	0.44
P <sub>2</sub> O <sub>5</sub>	1	0.52	0.52	0.48	0.58	0.29	0.48	0.28		0.71	0.54	0.14	18.3
LOI	1.88	1.76	0.22	1.6	1.74	2.23	0.75	1.32	0.41	0.41	1.74	2.24	
Total	100.47	101.3	100.01	100.51	1.74	100.95	100.65	101.15	99.95	0.41	100.32	101.3	
Mg#	44	47	43	47		30	52	39		52	31	20	

\* Total Fe as Fe<sub>2</sub>O<sub>3</sub>; DL = detection limit.

**Table 2**

Trace element data (ppm) for basaltic lavas from the Kessem and Megezez area.

Type	Kesem alkali basalt				Megezez						Standard (this analysis)		DL
					Transitional basalt				Trachy-andesite				
	Sample	KB9	KB12	KB13	KB14	MB3	MB7	MB10	MB11	MB1	MB4	OREAS 102a	
<b>Easting (m)</b>	564,823	557,343	558,123	564,525	552,925	551,123	553,947	553,590	554,725	553,905			
<b>Northing (m)</b>	1,004,655	1,005,259	1,007,110	1,009,462	1,021,113	1,017,885	1,024,135	1,019,203	1,017,999	1,020,806			
<b>Elev. (m)</b>	1720	2129	2193	2427	3026	3019	3395	3420	3078	3007			
<b>V</b>	200	315	304	308	283	352	284	403	56	32	36	349	
<b>Cr</b>	20	50	40	30	10	80	20	70	20	20	50	100	0.15
<b>Rb</b>	23.6	31.3	18.6	18.2	22.5	12.4	21.7	14.3	47.4	72.3	240	10	
<b>Sr</b>	751	1025	883	749	665	417	548	500	700	651	37.5	3540	
<b>Y</b>	35.3	28.6	26.1	24.4	39.5	21.6	34.5	23.4	46.9	44.7	97	422	0.02
<b>Zr</b>	259	242	212	203	279	144	235	164	321	344	329	1100	0.04
<b>Nb</b>	33.7	36.5	28.9	27.4	33.5	19.4	33.9	20.3	38.7	39.8	32	>2500	
<b>Cs</b>	0.15	0.14	0.09	0.13	0.1	0.04	0.12	0.03	2.07	1.46	3.05	0.34	
<b>Ba</b>	574	460	500	407	511	189	292	174.5	792	870	362	2580	0.07
<b>La</b>	35.8	30.6	27.5	26	36.6	16.6	28.2	18.4	48	49.4	293	3280	0.00
<b>Ce</b>	79.6	68.5	60.7	56.5	66.9	37.1	61.5	36.9	95.3	102	595	8090	0.01
<b>Pr</b>	11.00	9.22	8.37	7.9	10.5	5.12	8.69	5.37	13.3	13.75	53.3	>1000	0.00
<b>Nd</b>	51.00	41.7	38.7	36.7	46.6	24.3	40.4	25.2	61.9	60.2	181	4310	0.01
<b>Sm</b>	11.10	8.65	8.55	7.99	10.95	6.05	8.87	6.17	13.2	13.5	26.6	606	0.03
<b>Eu</b>	3.20	2.62	2.32	2.3	3.24	1.82	3.02	1.92	3.5	3.58	3.56	141.5	0.01
<b>Gd</b>	10.10	8.83	7.54	7.39	10.95	6.60	9.92	6.32	13.00	12.3	19.7	364	0.01
<b>Tb</b>	1.34	1.12	1.00	1.00	1.54	0.87	1.28	0.93	1.66	1.66	2.7	33.5	0.01
<b>Dy</b>	8.13	6.21	5.51	5.66	8.66	5.09	7.87	5.1	9.91	10.65	17.55	139.5	0.03
<b>Ho</b>	1.30	1.10	1.11	0.92	1.58	0.99	1.42	0.97	1.82	1.8	3.5	17.4	0.07
<b>Er</b>	3.67	3.11	2.94	2.7	4.15	2.54	3.86	2.66	4.81	5.25	11.25	36.8	0.03
<b>Tm</b>	0.41	0.34	0.32	0.31	0.49	0.26	0.46	0.30	0.63	0.63	1.51	3.38	0.01
<b>Yb</b>	2.39	2.12	2.04	2.04	2.83	1.66	2.62	1.82	3.52	3.57	10	17.9	0.04
<b>Lu</b>	0.36	0.31	0.29	0.28	0.42	0.28	0.39	0.25	0.54	0.59	1.57	2.02	0.04
<b>Hf</b>	6.1	6.0	5.3	5.4	7.5	4.2	6.4	4.8	7.6	8.8	9.3	25.2	0.06
<b>Ta</b>	5.9	5.9	4.2	2.7	2.7	1.7	2.8	1.9	3.7	4.0	2.6	11.3	0.08
<b>Th</b>	2.87	3.20	2.46	2.47	3.25	1.92	3.26	1.92	6.40	8.20	35.6	493	4.69
<b>U</b>	0.77	0.88	0.67	0.62	0.50	0.60	0.85	0.52	1.60	2.07	692	22.1	0.03

basalt field, but two samples fall in the trachy-andesite field. Samples from the Kessem Oligocene basalts are alkaline, whereas samples from the Megezez Miocene basalts and trachy-andesites are transitional with alkaline affinity (Fig. 6a). As shown in Fig. 6b, the Megezez Miocene basalts plot within the limits of the Ethiopian transitional basalts field defined by Ref. [28]. In contrast, the Kessem Oligocene basalts distinctly fall in the field of alkaline basalts. However, on the volcanic classification diagram of [29] using immobile elements (Nb/Y vs. Zr/TiO<sub>2</sub> × 0.0001), all samples fall in the field of alkaline basalts (Fig. 6c), where the Megezez Miocene basalts plot towards the boundary of sub-alkaline basalts rather than Kessem Oligocene basalts. Therefore, based on their chemical composition, samples of the study area are classified into two major groups; Kessem alkali basalts (Oligocene) and Megezez transitional basalts (Miocene).

5.2. Major elements

Whole-rock major element data for the Kessem alkali and Megezez transitional basalts are presented in Table 1. Kessem alkali basalts have a limited MgO range (4.92–5.91 wt %) and a lower SiO<sub>2</sub> (45.7–47.1 wt %) than Megezez transitional basalts (SiO<sub>2</sub> = 45.6–49.1 wt %; MgO = 4.06–7.06 wt %). The major element variation diagrams are shown in Fig. 7a–h. The Kessem alkali basalts and Megezez transitional basalts to trachy-andesites K<sub>2</sub>O, Na<sub>2</sub>O and Al<sub>2</sub>O<sub>3</sub> are negatively correlated with MgO, while CaO is positively correlated with MgO.

For the Kessem alkali basalts, TiO<sub>2</sub> is positively correlated with MgO. However, TiO<sub>2</sub> is negatively correlated with MgO for the Megezez transitional basaltic samples and sharply decreases toward the trachy-andesite samples. Fe<sub>2</sub>O<sub>3</sub> is positively correlated with MgO in the Kessem alkali basalts, whereas it remains constant among Megezez transitional basalts and sharply decreases for the trachy-

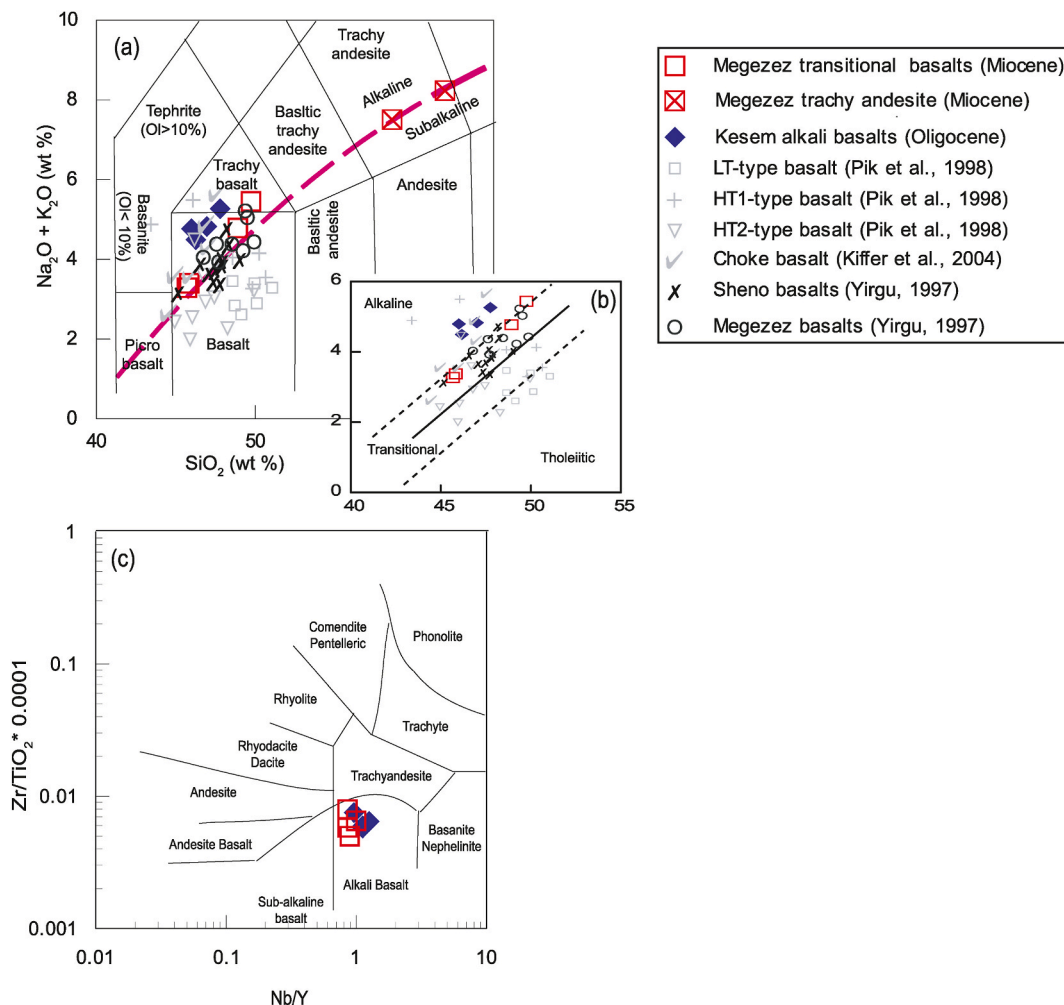
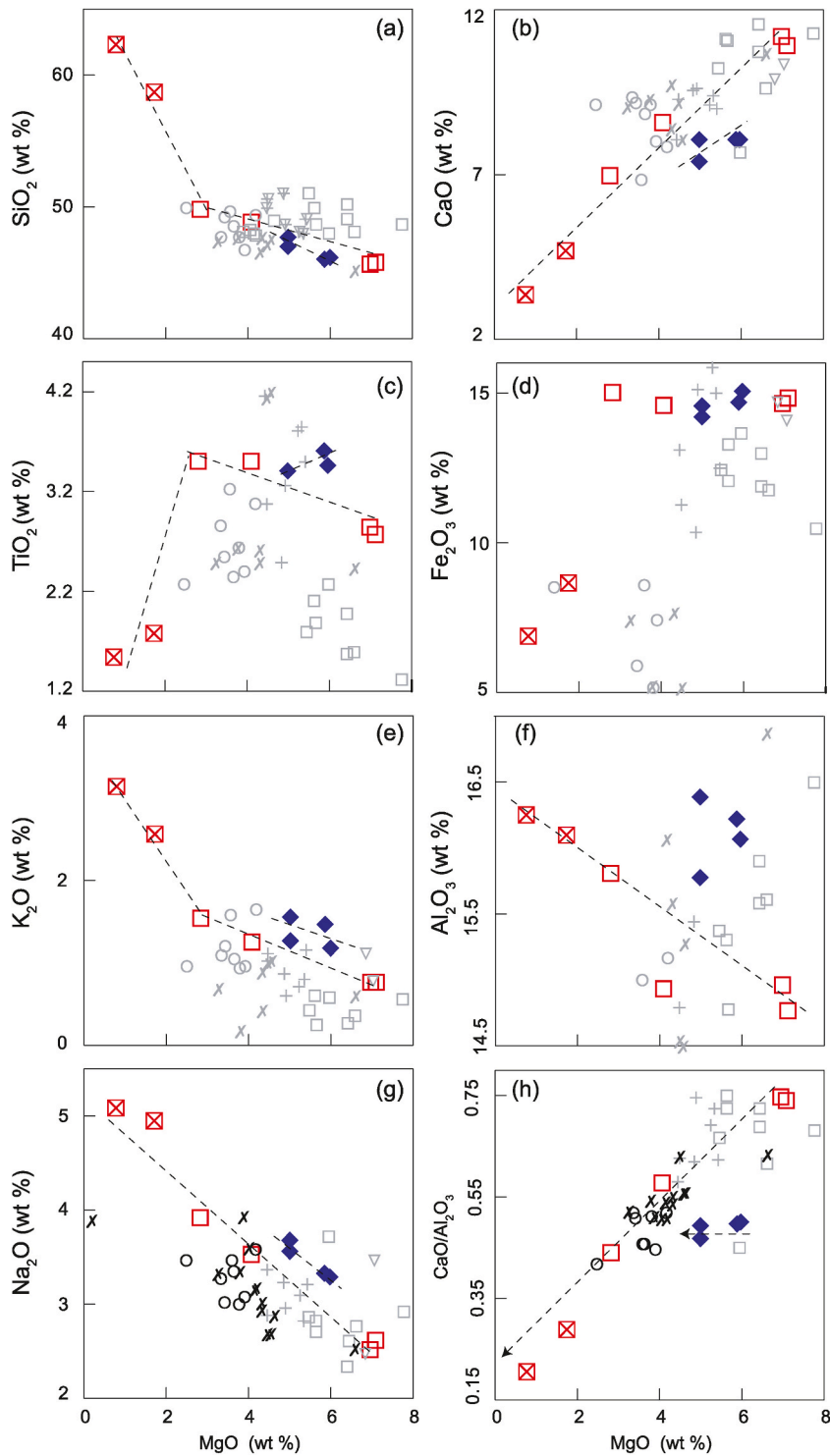


Fig. 6. a) Total alkali (Na<sub>2</sub>O + K<sub>2</sub>O) versus SiO<sub>2</sub> diagram [49] of the Kessem-Megezez basaltic rocks, b) The Ethiopian transitional basalts field defined by Ref. [28] and c) Volcanic classification diagram of [29] using immobile elements (Nb/Y vs. Zr/TiO<sub>2</sub> × 0.0001). Data for LT- and HT2-type basalts are from Refs. [8,9], Sheno and Megezez basalts from Ref. [14] are plotted for comparison. The dividing line of alkaline and sub alkaline is from Ref. [50].

andesites. On the other hand,  $\text{CaO}/\text{Al}_2\text{O}_3$  against  $\text{MgO}$  shows different trends for the two basalts. In the Kesem alkali basalt, as  $\text{MgO}$  decreases  $\text{CaO}/\text{Al}_2\text{O}_3$  shows a nearly constant horizontal trend. However, in the Megezez transitional basalts, the  $\text{CaO}/\text{Al}_2\text{O}_3$  ratio is positively correlated with  $\text{MgO}$ .



**Fig. 7.** Variation diagram of major elements vs  $\text{MgO}$  (wt %) of samples from Kesem-Megezez area. Data for LT- and HT2-type basalts are from Refs. [8,9], Sheno and Megezez basalts from Ref. [14] are plotted for comparison. Symbols as in Fig. 6.

5.3. Trace elements

The whole-rock trace element data are presented in Table 2. The incompatible trace element plots of Rb, Ba, Zr, Y, and Nb against MgO display different trends for both the Kesem alkali and Megezez transitional basalts (Fig. 8a–f and 9a–f). Rb, Ba, Zr, Y, and Nb correlate negatively with MgO. Moreover, the trace elements Yb and Th display a positive correlation with Zr in both groups. Whereas, V vs. Zr plot shows negative correlation for both groups. Furthermore, some of the incompatible trace elements against compatible elements Cr and MgO show distinctive trends for the two groups, e.g., Ce vs. Cr and MgO, Ba vs. MgO, Sr vs. MgO. In addition, Sr vs. Zr also shows two different positive trends; the Kesem alkali basalt shows a steep trend, while the Megezez transitional basalt to trachy-andesite shows a gentle slope. Trace element Ce against MgO in the Kesem alkali basalt shows a steep trend within a limited range of MgO, while the Megezez transitional basalt to trachy-andesite shows a gentle slope. For Ba versus MgO, the two groups exhibit parallel but separate trends.

As shown in Fig. 10a and b, the overall patterns of primitive mantle normalized trace elements for both the Kesem alkali and Megezez transitional basalts are similar to oceanic island basalts (OIB-type) and enriched asthenospheric mantle (E-MORB). The patterns show incompatible element enrichment and compatible element depletion. Both basaltic groups are significantly enriched in HFSE (Nb and Ta) than the LILE and LREE (La and Ce), which is a typical feature of OIB-like patterns [30]. Generally, in both basaltic groups, peaks in Ta and Ba and a trough in Th are observed. The trachy-andesite samples, MB1 and MB4 from the Megezez transitional group, show highly enriched in incompatible elements and depleted in Nb, Sr, and Ti.

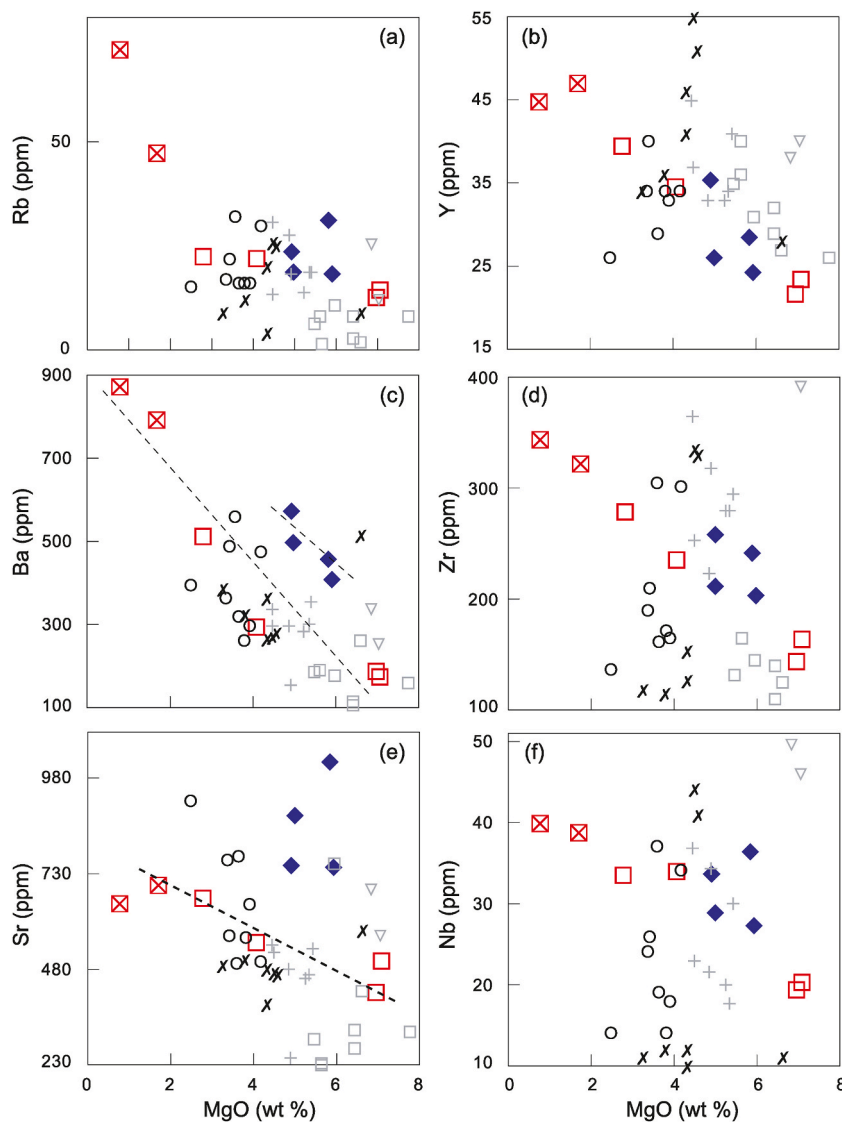


Fig. 8. Selected trace element plots against MgO (wt. %) of the study area. Data for LT- and HT2-type basalts are from Refs. [8,9], Sheno and Megezez basalts from Ref. [14] are plotted for comparison Symbols as in Fig. 6.

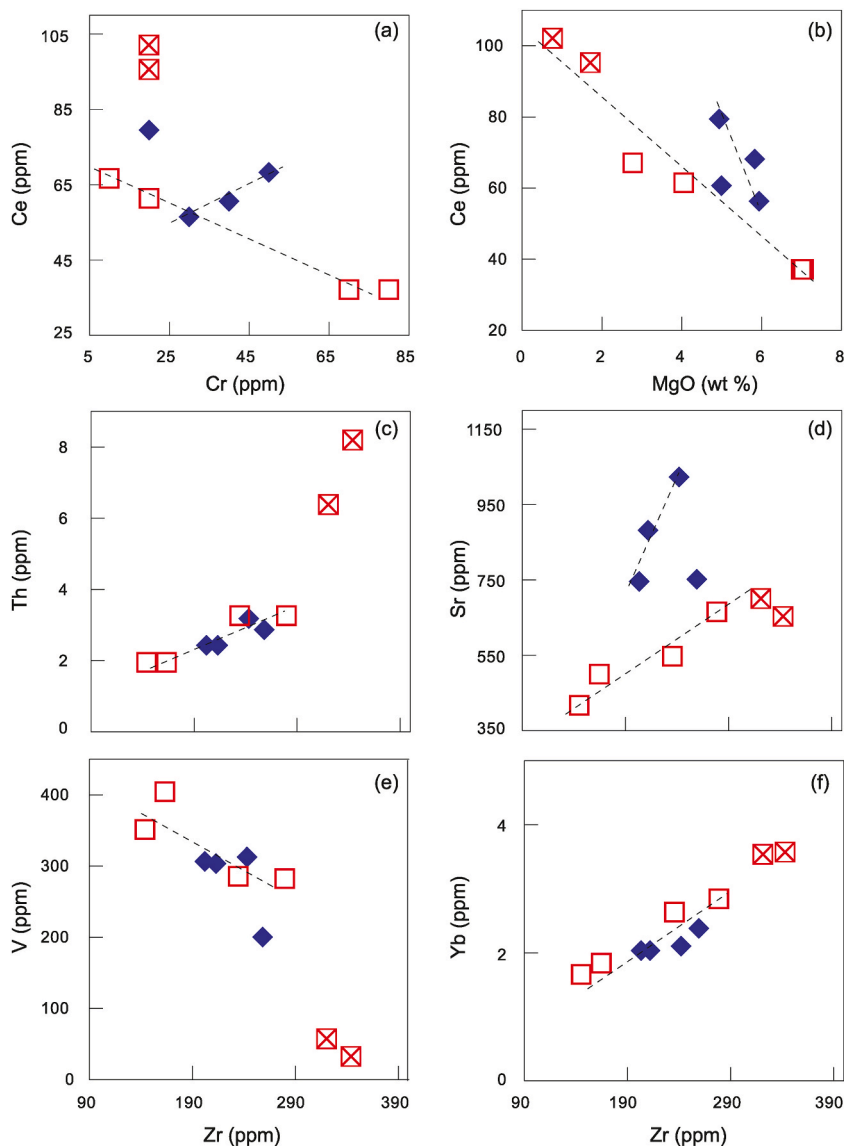


Fig. 9. Selected trace element plots against Cr, Zr in ppm and MgO (wt. %) of the study area. Symbols as in Fig. 6.

As shown in Fig. 10c and d, the chondrite-normalized rare earth element (REE) patterns of the Kesem alkaline and Megezez transitional basalts show enrichment in light rare earth elements (LREE) relative to heavy rare earth elements (HREE). These characteristic features are similar to those of ocean island basalt (OIB-type) [31]. In contrast, the Megezez transitional basalts show less enrichment in light rare earth elements (LREE), with an affinity of E-MORB compared to the Kesem alkaline basalts (Fig. 10d). The Kesem alkali basalts have LREE/HREE ( $La/Yb_N = 9.1\text{--}10.7$ ), MREE/HREE ( $Tb/Yb_N = 2.2\text{--}2.54$  and  $Dy/Yb_N = 1.8\text{--}2.27$ ) and LREE/MREE ratios ( $La/Sm_N = 2.07\text{--}2.3$ ). Megezez transitional basalts also show LREE/HREE ( $La/Yb_N = 7.17\text{--}9.28$ ), MREE/HREE ( $Tb/Yb_N = 2.11\text{--}2.38$  and  $Dy/Yb_N = 1.8\text{--}2.05$ ) and LREE/MREE ( $La/Sm_N = 1.77\text{--}2.36$ ).

## 6. Discussion

The petrographic and geochemical results of the Kesem-Megezez section reveal two distinct categories of basalts; 1) Kesem alkali basalts and 2) Megezez transitional basalts. The Kesem alkali basalts are part of the northwestern Ethiopian Plateau flood basalts, which are Oligocene in age. In contrast, the Megezez transitional basalts are part of the northwestern plateau shield basalts, which are Miocene in age. Generally, the geochemical characteristics of Kesem basalts are correlated with those of Sheno basalts [14] and HT1-type basalts [8,9], whereas, the Megezez basalts correlate with Choke basalts [1,37] and HT1-type basalts [8,9]. The Kesem and Megezez basalts are part of the Aiba and Tarmaber-Megezez formations, respectively [32–34].

The observed geochemical (major and trace element) variations between the Kesem alkali and Megezez transitional basalts may

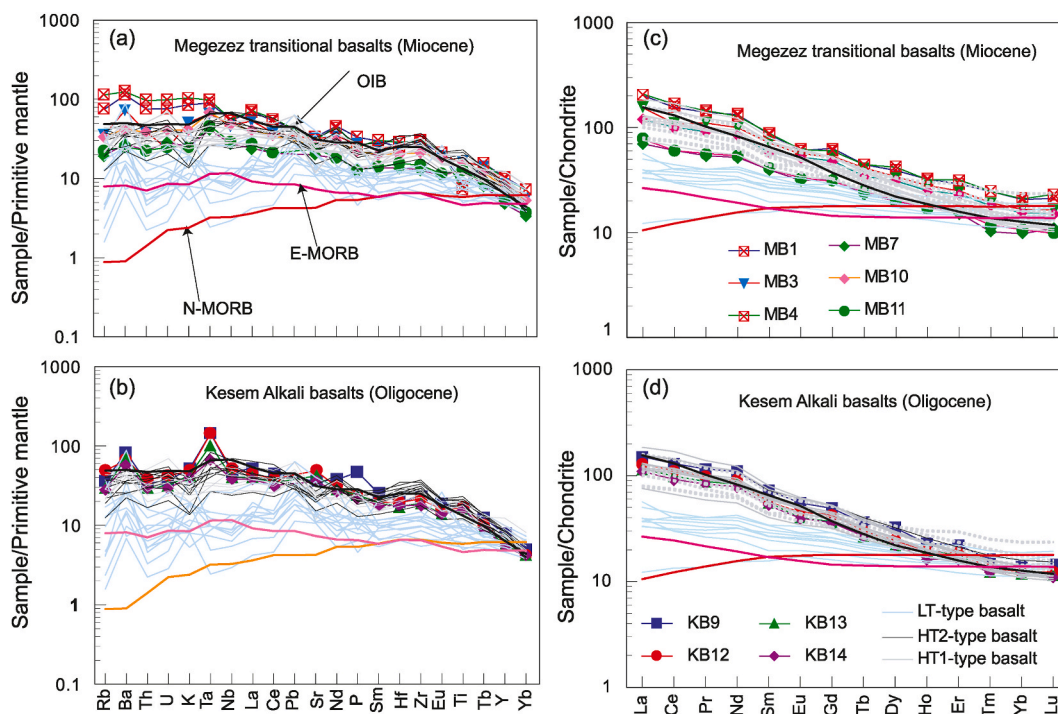


**Fig. 10.** Multi-element primitive mantle-normalized patterns (a and b) and Chondrite-normalized REE Patterns (c and d) of the study area. Normalization values of OIB, E-MORB and N-MORB are from Ref. [31]. Previous data for LT, HT1 and HT2-type basalts are from Ref. [8].

have been caused by the magma evolution process, the variable contribution from crustal materials, and/or from their mantle source. The compositional difference between the Kesem alkali and Megezez transitional basalts may indicate either magmatic processes or the nature of the mantle sources in their petrogenesis. The sources of their compositional variations are discussed below by assessing the possible magmatic processes (fractional crystallization, crustal contamination and the degree of partial melting and depth of melt segregation) and their mantle source features.

### 6.1. The role of fractional crystallization

The Kesem alkali and Megezez transitional basalts show low MgO and Cr contents (Kesem alkali basalt Cr = 50 ppm and MgO = 4.92–5.91 wt %; Megezez transitional basalt Cr = 80 ppm and MgO = 2.78–7.07 wt %) as compared to mantle-derived primitive basalts [Cr > 1000 ppm, MgO = 10–15 wt %; 35]. The presence of such low contents of MgO and Cr in the studied samples suggests that both the Kesem alkali basalts (Oligocene) and Megezez transitional basalt (Miocene) have undergone some degree of fractionation from their parent magmas.

As shown in Figs. 7b, c, e–h, 8c and e, and 9a, the major and incompatible trace element plots against MgO and Cr show clear distinctive trends for the Kesem alkali basalts and Megezez transitional basalts. This suggests that the Kesem Alkali basalts and Megezez transitional basalts were not differentiated by a similar fractional crystallization process. For instance,  $\text{Al}_2\text{O}_3$  against MgO in Kesem alkali basalt shows a steep trend within a limited range of MgO, whereas the Megezez transitional basalt to trachy-andesite shows a gentle slope.  $\text{Al}_2\text{O}_3$  is higher in the Kesem alkali basalts than in the Megezez transitional basalts for the same MgO values. Sr against MgO shows a positive trend in Kesem alkali basalts but a negative trend in Megezez transitional basalts. The trace element Ce against MgO and Sr against Zr in the Kesem alkali basalt shows a steep trend, whereas the basalt to trachy-andesite shows a gentle trend. In plots of CaO,  $\text{K}_2\text{O}$ ,  $\text{Na}_2\text{O}$  and Ba versus MgO, parallel but different trends are observed in the Kesem alkali and Megezez transitional basalts.

In both the Kesem alkali and Megezez transitional basalts to trachy-andesites,  $\text{Al}_2\text{O}_3$  is negatively correlated with MgO, while CaO is positively correlated with MgO, suggesting fractionation of olivine and pyroxene with insignificant plagioclase fractionation. On the other hand,  $\text{CaO}/\text{Al}_2\text{O}_3$  against MgO shows different trends for the Kesem alkali and Megezez transitional basalts. In the Kesem alkali basalts, as MgO decreases,  $\text{CaO}/\text{Al}_2\text{O}_3$  shows a nearly horizontal trend, implying that olivine is the dominant fractionation phase. However, in the Megezez transitional basalts, the  $\text{CaO}/\text{Al}_2\text{O}_3$  ratio decreases as MgO decreases, indicating that both pyroxene and olivine minerals were the dominant fractionated phases. Based on the petrographic descriptions of the Megezez basalts, the major crystallization phases are olivine, oxides, plagioclase and clinopyroxene (Fig. 5), in agreement with the above discussions. There are slight positive  $\text{TiO}_2$  variations with MgO among the Kesem alkali basalts. However,  $\text{TiO}_2$  increases with decreasing MgO for the Megezez transitional basalts and sharply decreases toward the trachy-andesite, indicating titanomagnetite fractionation in the Kesem

basalts but not in the Megezez transitional basalts.  $\text{Fe}_2\text{O}_3$  also decreases with decreasing of MgO only in the Kesem alkali basalts, but remains constant among the Megezez transitional basalts supporting the fractionation of titanomagnetite in the Kesem alkali basalts but not in the Megezez transitional basalts. The petrographic descriptions also support this inference of no titanomagnetite fractionation in the Megezez transitional basalts since opaque minerals are observed only as groundmass (Fig. 5).

Therefore, these compositional variations between the Kesem alkali and Megezez transitional basalts may demonstrate that the Kesem alkali and Megezez transitional basalts are different and that their compositional variations might not be explained by similar fractional crystallization processes.

### 6.2. The role of crustal contamination

The variations in major and incompatible trace element compositions between the Kesem alkali and Megezez transitional basalts possibly indicate variable contributions of crustal components and/or mantle sources to their genesis.

Incompatible trace element ratios such as La/Nb, Nb/U, K/Nb, and Ba/Nb are commonly used to distinguish uncontaminated oceanic basaltic rocks (MORB/OIB) from basalts contaminated by the continental crust [30,36]. The average Nb/U ratio of oceanic basalt is  $47 \pm 10$  [36], whereas that of continental crust is  $\sim 25$  [37]. Therefore, the Kesem alkali and Megezez transitional basalts were probably not affected by crustal contamination because the Nb/U ratios of the Kesem alkali basalt (Nb/U = 41.4–44.1) and Megezez transitional basalt (Nb/U = 32.3–67) are in the range of mantle-derived oceanic basalts (MORB/OIB). However, the two trachy-andesite samples from the Megezez area (MB1 and MB4) have Nb/U ratio of 24.18 and 19.2, respectively, indicating significant crustal contamination. According to Weaver [30], the trace element ratios for crustal materials are La/Nb = 2.2, Ba/Nb = 54 and Ba/La = 25. In contrast, the ratios in mantle-derived oceanic basalt are La/Nb (0.66–1.32), Ba/Nb (4.3–17.8) and Ba/La (4–16.6). The Kesem alkali basalt (La/Nb = 0.83–1.24, Ba/Nb = 12.6–17.3 and Ba/La = 15.03–16.03) and the Megezez transitional basalts (La/Nb = 0.83–1.09, Ba/Nb = 8.6–15.2 and Ba/La = 9.08–13.9) show values within the range of mantle-derived basalts. Therefore, there is no crustal material contribution to the petrogenesis of the Kesem alkali and Megezez transitional basalts. However, the two trachy-andesite samples from Megezez (Ba/Nb = 20.4 for MB1 and Ba/Nb = 21.8 for MB4) reflect crustal material contributions. As shown in Fig. 11a and b, except for the two trachy-andesite samples, the Kesem alkali and Megezez transitional basalts plotted in the field of oceanic island basalts (OIB). Furthermore, there are no trends toward the upper continental or lower crust [38,39], suggesting that there is no crustal contribution to the genesis of the Kesem alkali and Megezez transitional basalts.

In conclusion, the available trace element evidences indicate that the Kesem alkali and Megezez transitional basalts show no or insignificant involvement of crustal contamination in their genesis. As a result, the incompatible trace element variations suggest that crustal contamination is not the cause of the compositional variations in the Kesem alkali and Megezez transitional basalts.

### 6.3. Degree partial melting and depth of melt segregation

The compositional variations between the Kesem alkali basalts and Megezez transitional basalts may be due to the variable magma segregation depth and degree of partial melting of the homogenous mantle source. The Kesem alkali basalts show relatively wider ranges of Gd/Yb (3.62–4.2) and La/Yb ratios (12.7–14.9), whereas the Megezez transitional basalts show narrow ranges of Gb/Yb (3.4–3.9) and La/Yb ratios (10–13.8). The Megezez transitional basalts may have been derived from a relatively shallow depth with a higher degree of partial melting than the Kesem alkali basalts (Fig. 12a). As shown in Fig. 12b, the Kesem alkali and Megezez transitional basalts may have been derived from a mantle source within the stability field of garnet at depths greater than 80 km [40,41].

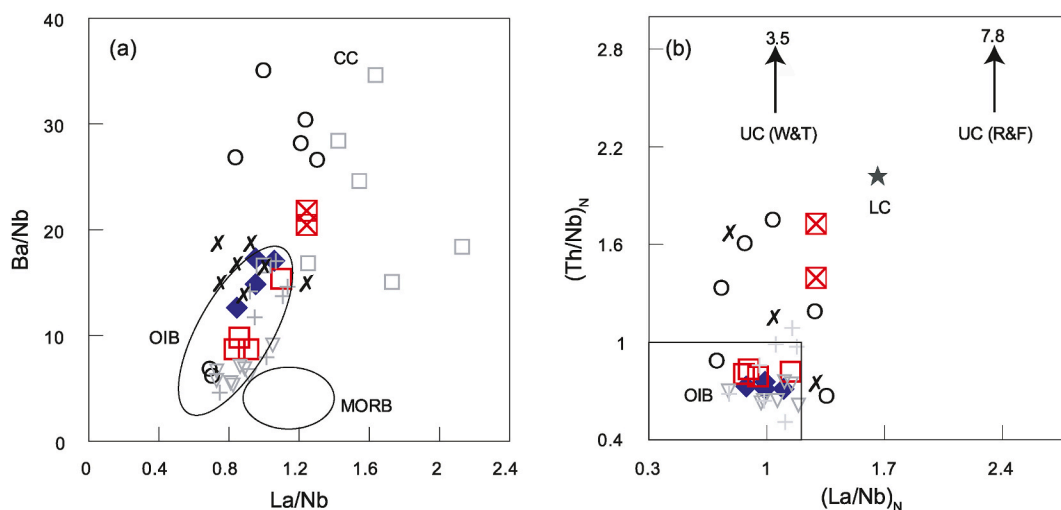


**Fig. 11.** (a) La/Nb vs Ba/Nb, (b)  $(\text{La}/\text{Nb})_N$  vs  $(\text{Th}/\text{Nb})_N$ , (c) MgO vs. Ba/Nb, and (d) Zr/Nb vs Ba/Nb ratios. The fields for OIB and MORB are taken from Ref. [51]. Reference values for upper crust (UC) and lower crust (LC) are taken from (R&F) [39] and (W&T) [38]. Symbols as in Fig. 6.

A non-modal equilibrium melting model of the spinel- and garnet-bearing lherzolitic mantle source using primitive mantle [31] as a starting source was used to assess the melting conditions of the Kesem alkali and Megezez transitional basalts. As shown in  $(\text{Sm}/\text{Yb})_N$  versus  $(\text{La}/\text{Sm})_N$ , the Kesem alkali basalt can be produced by melting of ~3–4% residual garnet with a 2–3% degree of partial melting. Whereas, the Megezez transitional basalts are formed by melting of ~2–3% residual garnet with >3% degree of partial melting (Fig. 12c).

#### 6.4. Mantle source characteristics

The primitive mantle-normalized multi-element, and chondrite-normalized REE patterns of the Kesem alkali and Megezez transitional basalts are generally more similar to the OIB-like patterns (Fig. 10). The Megezez group shows a slight tendency towards the E-MORB pattern. The enrichment of LREE relative to MREE and HREE, as well as the fractionation of MREE from HREE, indicate that the source of the Kesem alkali basalts (Oligocene) and the Megezez transitional basalts (Miocene) were located in deep mantle sources with a garnet stability field (Fig. 10).

As shown in Fig. 13a and b, Nb/Zr versus Rb/Zr and Ba/Zr plots demonstrate that both the Kesem alkali basalt and Megezez transitional basalt fall inside the mantle array between oceanic island basalt (OIB) and enriched mid-oceanic ridge basalt (E-MORB), [31]. It is also shown in K/Nb versus Zr/Nb (Fig. 13c) and Th/Yb versus Nb/Yb plots (Fig. 13d) where all basalts plot between the values of the OIB and E-MORB mantle components. In the Th/Yb versus Nb/Yb (Fig. 13d) plot, the Kesem alkali basalts (Oligocene) display a greater tendency towards the OIB mantle component, whereas the Megezez transitional basalts (Miocene) show a greater tendency towards the E-MORB mantle component. These features are also observed in the REE and multi-element patterns in Fig. 10a

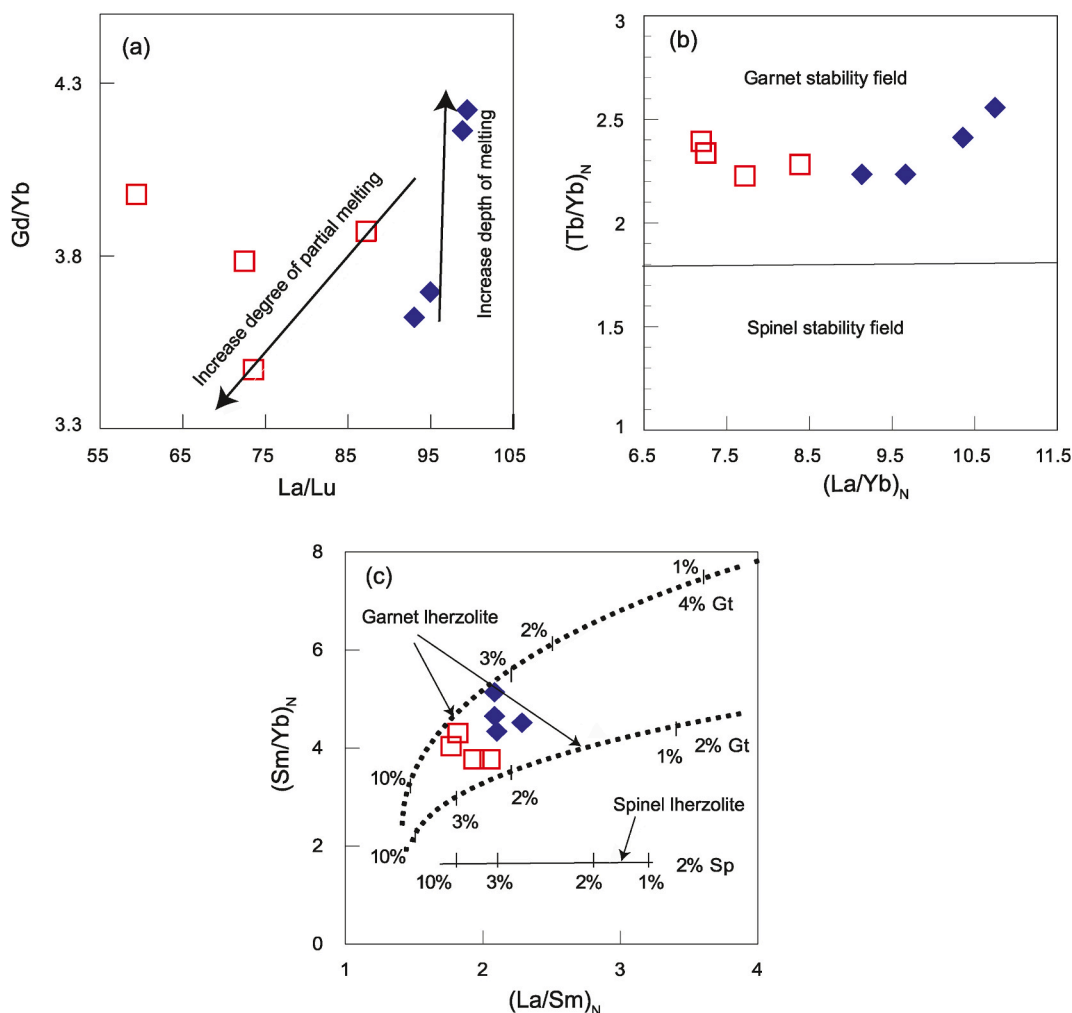


**Fig. 12.** a) Gd/Yb versus La/Lu b)  $(\text{Tb}/\text{Yb})_N$  versus  $(\text{La}/\text{Yb})_N$  plots and c) Non-modal batch melting modeling of a lherzolitic mantle source,  $(\text{Sm}/\text{Yb})_N$  versus  $(\text{La}/\text{Sm})_N$  plot. The degree of partial melting is indicated by the tick marks. Garnet and Spinel-bearing lherzolite mantle sources are taken from Refs. [52,53]. Normalization values are from Ref. [31]. Stability fields of Garnet and Spinel in Figure b is taken from Ref. [41]. Symbols as in Fig. 6.

and b.

Therefore, from the observed trace element patterns and ratios, the Kesem alkali and Megezez transitional basalts are more likely to be derived from the mixing of two mantle components in various proportions: 1) mantle plume (OIB) and 2) an enriched asthenospheric mantle (E-MORB). The basalts in both groups fall along a mixing line between the OIB and the E-MORB (Fig. 13d). The linear trend along the average OIB and E-MORB in the Kesem and Megezez basalts indicates a possible interaction of the OIB-type plume with the E-MORB component melt in their source origins, with a dominant proportion of plume component (OIB) during the Oligocene (OIB = 55–75%; EMORB = 25–45%), but an equal proportion of OIB and enriched asthenosphere (E-MORB) in the Miocene (OIB = 40–60%; EMORB = 40–60%), (Fig. 13d).

The results of this investigation demonstrate that mantle plume (OIB) and metasomatized N-MORB (EMORB) components play a significant role in the genesis of Oligocene flood basalts and Miocene shield basalts in the Ethiopian plateau. However, previous investigations of various parts of the Ethiopian Plateau magmatism inferred contributions of the depleted asthenospheric mantle (N-MORB) and lithospheric mantle [8,9,42,43], heterogeneous upper mantle plume upwelling [1], or interaction of an asthenospheric mantle and EM-like subcontinental lithospheric mantle [SCLM; 44].

Based on the above-discussed geochemical evidence, the following scenario explains the genesis of basalts from Oligocene and Miocene magmatism in the Ethiopian Plateau. Magmatism began with the arrival of a mantle plume (OIB; aka Afar Plume) that came across a sub-lithospheric geochemically enriched and fertile asthenospheric mantle component (E-MORB). The enriched asthenospheric mantle component (E-MORB) possibly originated from an earlier depleted mantle wedge (N-MORB) that was metasomatized and enriched by subduction fluid/sediment during the Neoproterozoic subduction history of the region [45,46]. Alternatively, the E-MORB component may originate from plume- entrained blobs/lenses of mantle components from a depth below the asthenosphere [47]. Thus, the uprising of a hot mantle plume that impinging beneath the lithosphere at ~30 Ma [9] generates OIB-type melts due to decompression. Simultaneously, the thermal effect of the hot plume also triggered the melting of the fertile E-MORB component in the asthenosphere at the garnet stability depth. Then, the interaction between more melts from the plume (OIB) and lesser melts from the E-MORB created flood basalts (Kesem basalts). During the Miocene, progressive melting of the OIB and E-MORB generated the plateau

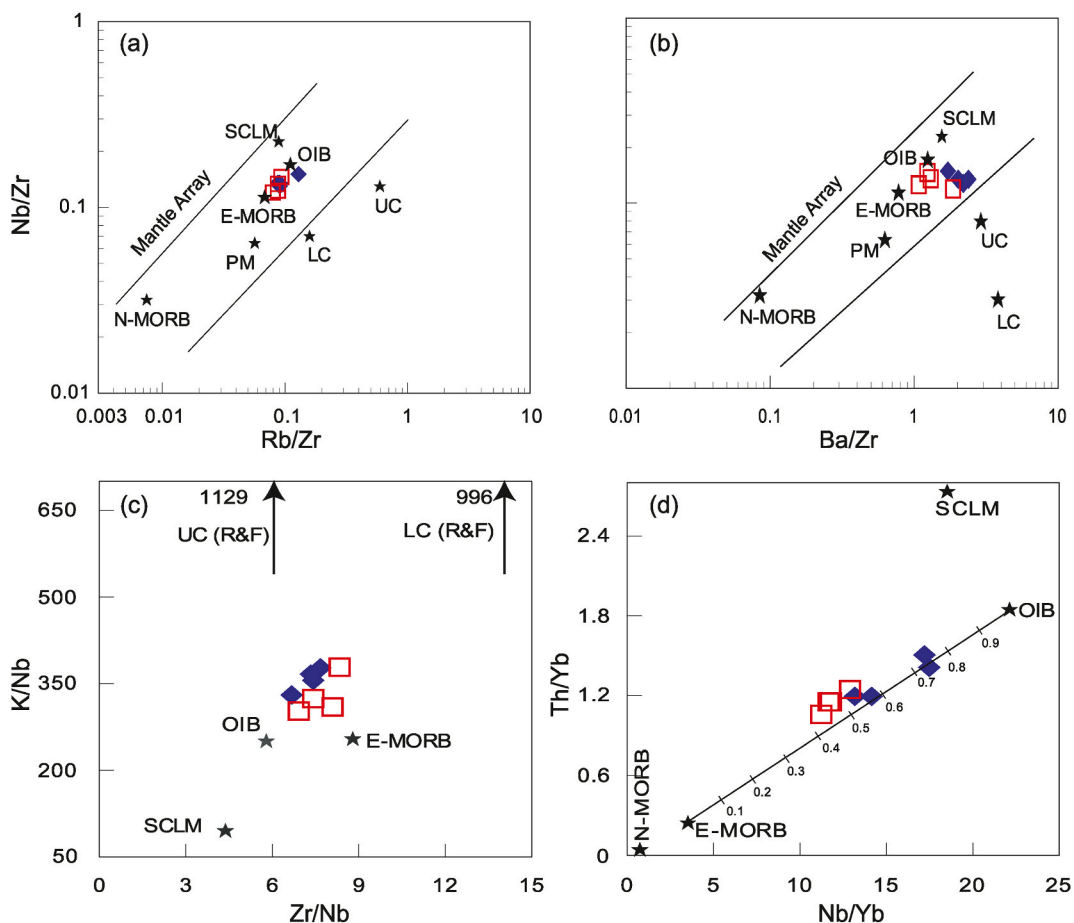


**Fig. 13.** Trace element ratio plot of the basaltic samples of the study area. (a) Rb/Zr vs Nb/Zr, (b) Ba/Zr vs Nb/Zr, (c) Zr/Nb vs K/Nb and (d) Th/Yb vs Nb/Yb. The solid line represent simple binary mixing model between OIB and EMORB, and the ticks indicate proportions of the two mantle components. Mantle values taken from Ref. [31]. Upper (UC) and Lower Continental Crust (LC) values are from R&F [39].

shield basalts (Megezez basalts).

## 7. Conclusions

This study covers both the Oligocene flood and Miocene shield basalts from the Kesem-Megezez section. Kesem alkali basalts (Oligocene) are aphyric in texture and holocrystalline groundmasses containing olivine, pyroxene and plagioclase minerals with <1% plagioclase phenocrysts. The Megezez transitional basalts (Miocene) are phyric in texture and holocrystalline groundmass containing olivine, pyroxene and plagioclase minerals with 10%–20% of pyroxene, olivine and plagioclase phenocrysts. The Kesem and Megezez basalts are alkaline and transitional, respectively.

The geochemical variations in the Kesem alkaline basalts and the Megezez transitional basalts result from different depths of melting by variable degrees of partial melting. The Kesem alkali basalt can be produced by melting of ~3–4% residual garnet with approximately 3% degree of partial melting, whereas the Megezez transitional basalts are formed by melting of ~2–3% residual garnet with >3% degree of partial melting.

The results of this investigation demonstrate that mantle plume (OIB) and metasomatized N-MORB (EMORB) components play a significant role in the genesis of Oligocene flood basalts and Miocene shield basalts in the Ethiopian plateau. The interaction between more melts from the plume (OIB) and lesser melts from the E-MORB created the flood basalts (Kesem alkali basalts) of the Ethiopian plateau during the Oligocene (~30 Ma) and mixing between more melts from the E-MORB mantle and less plume component (OIB) generated the shield basalts (Megezez transitional basalts) in the plateau during the Miocene.

## Declarations

### *Author contribution statement*

Birhane Girum, Takele Chekol & Daniel Meshesha: Conceived and designed the experiments; Performed the experiments; Analyzed and interpreted the data; Contributed reagents, materials, analysis tools or data; Wrote the paper.

## Funding statement

This work was supported by Addis Ababa Science and Technology University (AASTU).

## Data availability statement

Data included in article/supplementary material/referenced in article.

## Additional information

No additional information is available for this paper.

## Declaration of competing interest

The authors declare that they have no known competing financial interests or personal relationships that could have appeared to influence the work reported in this paper.

## Acknowledgement

MSc program opportunity by Addis Ababa Science and Technology University (AASTU) was to BG. We also thank Addis Ababa Science and Technology University (AASTU) for providing necessary facilities and supports for the research work. For thin section preparation, we appreciate Central Laboratory of the Geological Survey of Ethiopia. Australian Laboratory Services (ALS) also acknowledged for providing the major and trace element analyses result on time.

## Appendix A. Supplementary data

Supplementary data to this article can be found online at <https://doi.org/10.1016/j.heliyon.2023.e17256>.

## References

- [1] B. Kieffer, N. Arndt, H. Lapiere, F. Bastien, D. Bosch, A. Pecher, G. Yirgu, D. Ayalew, D. Weis, D.A. Jerram, F. Keller, C. Meugniot, Flood and shield basalts from Ethiopia: magmas from the African superswell, *J. Petrol.* 45 (2004) 793–834.

- [2] E. Wolfenden, C. Ebinger, G. Yirgu, A. Deino, D. Ayalew, Evolution of the northern Main Ethiopian Rift: birth of a triple junction, *Earth Planet Sci. Lett.* 224 (2004) 213–228, <https://doi.org/10.1016/j.epsl.2004.04.022>.
- [3] J. Chorowicz, The East African rift system, *J. Afr. Earth Sci.* 43 (2005) 379–410, <https://doi.org/10.1016/j.jafrearsci.2005.07.019>.
- [4] C.J. Ebinger, N.H. Sleep, Cenozoic magmatism throughout east Africa resulting from impact of a single plume, *Nature* 395 (1998) 788–791.
- [5] R. George, N. Rogers, S. Kelley, Earliest magmatism in Ethiopia: evidence for two mantle plumes in one flood basalt province, *Geology* 26 (1998) 923–926.
- [6] A. Davidson, D. Rex, Age of volcanism and rifting in southwestern Ethiopia, *Nature* 283 (1980) 657–658.
- [7] C.J. Ebinger, T. Yemane, G. Woldegabriel, J.L. Aronson, R.C. Walter, Late Eocene-Recent volcanism and faulting in the southern main Ethiopian rift, *J. Geol. Soc., London* 150 (1993) 99–108.
- [8] R. Pik, C. Deniel, C. Coulon, G. Yirgu, C. Hofmann, D. Ayalew, The northwestern Ethiopian Plateau flood basalts: classification and spatial distribution of magma types, *J. Volcanol. Geoth. Res.* 81 (1998) 91–111.
- [9] R. Pik, C. Deniel, C. Coulon, G. Yirgu, B. Marty, Isotopic and trace element signatures of Ethiopian flood basalts; evidence for plume-lithosphere interactions, *Geochem. Cosmochim. Acta* 63 (1999) 2263–2279.
- [10] L. Beccaluva, G. Bianchini, C. Natali, F. Siena, Continental flood basalts and mantle plumes: a case study of the northern Ethiopian Plateau, *J. Petrol.* 50 (2009) 1377–1403.
- [11] K. Stewart, N. Rogers, Mantle plume and lithosphere contributions to basalts from southern Ethiopia, *Earth Planet Sci. Lett.* 139 (1996) 195–211.
- [12] K. Burke, J.M. Cannon, Plume-plate interaction, *Can. J. Earth Sci.* 51 (3) (2014), <https://doi.org/10.1139/cjes-2013-0115>.
- [13] B. Abebe, Quaternary faulting and volcanism in the main Ethiopian rift, *J. Afr. Earth Sci.* 48 (2007) 115–124, <https://doi.org/10.1016/j.jafrearsci.2006.10.005>.
- [14] G. Yirgu, Magma-crust interaction during emplacement of Cenozoic volcanism in Ethiopia: geochemical evidence from Sheno-Megeze area central Ethiopia, *Ethiop. J. Sci.* 20 (1) (1997) 40–72.
- [15] P. Mohr, B. Zanettin, The Ethiopian flood basalt province, *Continental Flood Basalts* (1988) 63–110, [https://doi.org/10.1007/978-94-015-7805-9\\_3](https://doi.org/10.1007/978-94-015-7805-9_3).
- [16] C. Hofmann, V. Courtillot, G. Féraud, P. Rochette, G. Yirgu, G.E. Ketefo, R. Pik, Timing of the Ethiopian flood basalt event and implications for plume birth and global change, *Nature* 389 (1997) 838–841, <https://doi.org/10.1038/39853>.
- [17] B. Zanettin, E. Justin-Visentin, M. Nicoletti, E.M. Piccirillo, Correlations among Ethiopian volcanic formations with special references to the chronological and stratigraphical problems of the “Trap Series”, *Atti. Conveg. Lincei* 47 (231) (1980) 252.
- [18] R.M.M. George, Thermal and Tectonic Controls on Magmatism in the Ethiopian Province, The Open University, 1997. Doctoral Dissertation.
- [19] T. Chernet, W.K. Hart, J.L. Aronson, R.C. Walter, New age constraints on the timing of volcanism and tectonism in the northern Main Ethiopian Rift–southern Afar transition zone (Ethiopia), *J. Volcanol. Geoth. Res.* 80 (3) (1998) 267–280.
- [20] T.M. Alemayehu, Petrography and Petrology of Gina Ager-Megeze Locality, Megeze Shield Volcanics North Shoa, Central Ethiopia, School of Graduate Studies. Addis Ababa University, Thesis, 2018.
- [21] I.A. Ukstins, P.R. Renne, E. Wolfenden, J. Baker, D. Ayalew, M. Menzies, Matching conjugate volcanic rifted margins: Ar/Ar chrono-stratigraphy of pre- and syn-rift bimodal flood volcanism in Ethiopia and Yemen, *Earth Planet Sci. Lett.* 198 (3–4) (2002) 289–306.
- [22] C. Natali, L. Beccaluva, G. Bianchini, F. Siena, Comparison among Ethiopia-Yemen, Deccan, and Karoo continental flood basalts of central Gondwana: insights on lithosphere versus asthenosphere contributions in compositionally zoned magmatic provinces, *Geol. Soc. Am. Spec. Pap.* 526 (2017) 191–215.
- [23] C. Deniel, P. Vidal, C. Coulon, P.J. Vellutini, P. Pigué, Temporal evolution of mantle sources during continental rifting: the volcanism of Djibouti (Afar), *J. Geophys. Res.* 99 (1994) 2853–2869.
- [24] D. Ayalew, C. Ebinger, E. Bourdon, E. Wolfenden, G. Yirgu, N. Grassineau, Temporal Compositional Variation of Syn-Rift Rhyolites along the Western Margin of the Southern Red Sea and Northern Main Ethiopian Rift, Geological Society, London, 2006, <https://doi.org/10.1144/GSL.SP.2006.259.01.10>. Special Publications.
- [25] B. Zanettin, Evolution of the Ethiopian volcanic province, *Ser* 9 (1) (1992) 156–181 (Accad. Naz. Lincei, Rome).
- [26] C. Ebinger, Continental break-up: the East African perspective, *Astron. Geophys.* 46 (2005) 16–21.
- [27] M. Bonini, G. Corti, I. Fabrizio, P. Manetti, F. Mazzarini, T. Abebe, Z. Pecskaý, Evolution of the Main Ethiopian Rift in the frame of Afar and Kenya rifts propagation, *Tectonics* 24 (2005), <https://doi.org/10.1029/2004TC001680>.
- [28] E.M. Piccirillo, E. Justin-Visentin, B. Zanettin, J.L. Joron, M. Treuil, Geodynamic evolution from plateau to rift: major and trace element geochemistry of the central eastern Ethiopian plateau volcanics, *Neues Jahrbuch Geol. Palaontol. Abhand.* 158 (1979) 139–179.
- [29] J.A. Winchester, P.A. Floyd, Geochemical discrimination of different magma series and their differentiation products using immobile elements, *Chem. Geol.* 20 (1997) 245–252.
- [30] B.L. Weaver, The origin of ocean island basalt end-member compositions: trace element and isotopic constraints, *Earth Planet Sci. Lett.* 104 (2–4) (1991) 381–397, [https://doi.org/10.1016/0012-821X\(91\)90217-6](https://doi.org/10.1016/0012-821X(91)90217-6).
- [31] S.S. Sun, W.F. McDonough, Chemical and isotopic systematics of oceanic basalts: implications for mantle composition and processes, *Geol. Soc., London, Special Publications* 42 (1989) 313–345.
- [32] B. Zanettin, E. Justin-Visentin, M. Nicoletti, E.M. Piccirillo, Correlations among Ethiopian volcanic formations with special references to the chronological and stratigraphical problems of the “Trap Series”, *Atti. Conveg. Lincei* 47 (231) (1980) 252.
- [33] P. Mohr, Ethiopian flood basalt province, *Nature* 303 (5918) (1983) 577.
- [34] S.M. Berhe, B. Desta, M. Nicoletti, M. Teferra, Geology, geochronology and geodynamic implications of the Cenozoic magmatic province in W and SE Ethiopia, *J. Geol. Soc.* 144 (2) (1987) 213–226.
- [35] A.W. Hofmann, K.P. Jochum, M. Seufert, W.M. White, Nb and Pb in oceanic basalts: new constraints on mantle evolution, *Earth Planet Sci. Lett.* 79 (1–2) (1986) 33–45, [https://doi.org/10.1016/0012-821X\(86\)90038-5](https://doi.org/10.1016/0012-821X(86)90038-5).
- [36] P.C. Hess, in: J. Phipps Morgan, D.K. Blackman, J.M. Sinton (Eds.), Phase Equilibria Constraints on the Origin of Ocean Floor Basalts, Mantle Flow and Melt Generation at Mid-Ocean Ridges, Geophysical Monograph Amsterdam Geophysical Union, 1992, pp. 67–102.
- [37] R.L. Rudnick, S. Gao, in: H.D. Holland, K.K. Turekian (Eds.), Composition of the Continental Crust, Treatise on Geochemistry, vol. 3, Elsevier, Amsterdam, 2004, pp. 1–64.
- [38] S.D. Weaver, J. Tarney, Empirical approach to estimating the composition of continental crust, *Nature* 310 (1984) 575–577.
- [39] R.L. Rudnick, D.M. Fountain, Nature and composition of the continental crust: a lower crustal perspective, *Rev. Geophys.* 95 (1995) 267–309.
- [40] E. Takahashi, I. Kushiro, Melting of a dry peridotite at high pressures and basalt magma genesis, *Am. Mineral.* 68 (1983) 859–879.
- [41] K. Wang, T. Plank, J.D. Walker, E.I. Smith, A mantle melting profile across the Basin and Range, SW USA, *J. Geophys. Res.* 107 (b1) (2002), <https://doi.org/10.1029/2001JB00209>.
- [42] W.K. Hart, G. Woldegabriel, R.C. Walter, S.A. Mertzman, Basaltic volcanism in Ethiopia: constraints on continental rifting and mantle interactions, *J. Geophys. Res.* 94 (1989) 7731–7748.
- [43] T. Furman, Geochemistry of East African rift basalts: an overview, *J. Afr. Earth Sci.* 48 (2007) 147–160, <https://doi.org/10.1016/j.jafrearsci.2006.06.009>.
- [44] D. Ayalew, S. Jung, R.L. Romer, D. Garbe-Schönberg, Trace element systematics and Nd, Sr and Pb isotopes of Pliocene flood basalt magmas (Ethiopian rift): a case for Afar plume-lithosphere interaction, *Chem. Geol.* 493 (2018) 172–188, <https://doi.org/10.1016/j.chemgeo.2018.05.037>.
- [45] T. Tamarat, T. Chekol, D. Meshesha, Petrology and geochemistry of basaltic rocks from north western Ethiopian plateau continental flood Basalt, *J. Afr. Earth Sci.* 182 (2021), 104282, <https://doi.org/10.1016/j.jafrearsci.2021.104282>.
- [46] D. Meshesha, T. Chekol, S. Negussia, Major and trace element compositions of basaltic lavas from western margin of central main Ethiopian rift: enriched asthenosphere vs. mantle plume contribution, *Heliyon* 7 (12) (2021), e08634, <https://doi.org/10.1016/j.heliyon.2021.e08634>.
- [47] D. Meshesha, R. Shinjo, Rethinking geochemical feature of the Afar and Kenya mantle plumes and geodynamics implications, *J. Geophys. Res. Solid Earth* 113 (9) (2008) 1–17, <https://doi.org/10.1029/2007JB005549>.
- [48] D. Meshesha, D. Hailmariam, A. Mamo, Compiled Geological Map of Debre Birhan Area, Geological Surveys of Ethiopia (GSE), 2009 (Unpublished).

- [49] M.J. Le Bas, R.W. Le Maitre, A. Streckeisen, B. Zanettin, A chemical classification of volcanic rocks based on the total alkali-silica diagram, *J. Petrol.* 27 (3) (1986) 745–750.
- [50] T.N. Irving, W.R.A. Baragar, A guide to the chemical classification of the common volcanic rocks, *Can. J. Earth Sci.* 8 (1971) 523–548.
- [51] R. Shinjo, T. Chekol, D. Meshesha, T. Taya, Y. Tatsumi, Geochemistry and geochronology of the mafic lavas from the southeastern Ethiopian rift (the East African Rift System): assessment of models on magma sources, plume-lithosphere interaction and plume evolution, *Contrib. Mineral. Petrol.* 162 (2011) 209–230.
- [52] F. Jourdan, H. Bertrand, U. Scha, Major and trace element and Sr, Nd, Hf, and Pb isotope compositions of the Karoo Large Igneous Province, Botswana and Zimbabwe: lithosphere vs mantle plume contribution, *J. Petrol.* 48 (6) (2007), <https://doi.org/10.1093/petrology/egm010>.
- [53] M. Grègoire, D.R. Bell, A.P. Le Roex, Garnet lherzolites from the Kaapvaal craton (South Africa): trace element evidence for metasomatized history, *J. Petrol.* 44 (4) (2003) 629–657.